NASA TECHNICAL NOTE

NASA TN D-6057

NASA TN D-6057

MEASURED ELECTRON CONVERSION RATIOS FOR THE 1064-keV GAMMA RAY OF BISMUTH-207

by Sherwin M. Beck

Langley Research Center
Hampton, Va. 23365

NATIONAL AERONAUTICS AND SPACE ADMINISTRATION • WASHINGTON, D. C. • NOVEMBER 1970

1. Report No.	2. Government Accession No.	3. Recip.
NASA TN D-6057		

4. Title and Subtitle

MEASURED ELECTRON CONVERSION RATIOS FOR THE 1064-keV GAMMA RAY OF BISMUTH-207

5. Report Date: November 1970

6. Performing Organization Code:

7. Author(s)

Sherwin M. Beck

8. Performing Organization Report No.: L-6015

9. Performing Organization Name and Address

NASA Langley Research Center
Hampton, Va. 23365

10. Work Unit No.: 124-09-21-01

11. Contract or Grant No.:

12. Sponsoring Agency Name and Address

National Aeronautics and Space Administration
Washington, D.C. 20546

13. Type of Report and Period Covered: Technical Note

14. Sponsoring Agency Code:

15. Supplementary Notes

16. Abstract

The electron conversion ratios for the 1064-keV gamma ray of bismuth-207 have been determined from the conversion electron spectra obtained by using lithium-drifted silicon (Si(Li)) detectors. The spectrometer system had an energy resolution between 4 and 5 keV at 1 MeV, which was sufficient to separate the L- and M-shell conversion electron lines. Sixty-one measurements were made with four Si(Li) detectors. The average values which were obtained for the conversion ratios of K-, L-, and M-shell electrons were $\frac{K}{L} = 3.90\ (\pm 0.03)$, $\frac{K}{M} = 11.23\ (\pm 0.22)$, $\frac{K}{L + M} = 2.90\ (\pm 0.03)$, and $\frac{L}{M} = 2.89\ (\pm 0.05)$. (The values in parentheses are the standard deviations.)

17. Key Words (Suggested by Author(s))	18. Distribution Statement
Electron conversion ratios Lithium-drifted silicon detectors Bismuth-207 Nuclear generators	Unclassified – Unlimited

19. Security Classif. (of this report)	20. Security Classif. (of this page)	21. No. of Pages	22. Price*
Unclassified	Unclassified	39	$3.00

*For sale by the Clearinghouse for Federal Scientific and Technical Information
Springfield, Virginia 22151

MEASURED ELECTRON CONVERSION RATIOS FOR THE 1064-keV GAMMA RAY OF BISMUTH-207

By Sherwin M. Beck
Langley Research Center

SUMMARY

The electron conversion ratios for the 1064-keV gamma ray of bismuth-207 (Bi^{207}) have been measured. The results from all measurements were combined to obtain the following weighted averages for the conversion ratios of K-, L-, and M-shell electrons: $\frac{K}{L} = 3.90\ (\pm 0.03)$, $\frac{K}{M} = 11.23\ (\pm 0.22)$, $\frac{K}{L+M} = 2.90\ (\pm 0.03)$, and $\frac{L}{M} = 2.89\ (\pm 0.05)$. (The values in parentheses are the standard deviations.)

The conversion ratios were corrected to eliminate those events caused by the simultaneous absorption of electrons and X-rays in the detectors. Compton events from the 1770-keV gamma ray and summed events from conversion electrons were negligible. The data were corrected to eliminate distortions caused by backscattered electrons.

The detectors were lithium-drifted silicon. These detectors were originally produced at the Langley Research Center for electron transmission studies at the NASA Space Radiation Effects Laboratory. The detectors and the associated electronics had an energy resolution between 4 and 5 keV for the 974-keV conversion electrons of Bi^{207} at 77 K; this resolution was sufficient to separate the L- and M-shell conversion electrons. Four 3-mm detectors were used. The voltage applied to the detectors ranged from 200 to 900 volts. Leakage currents were less than 10^{-9} ampere at 500 volts bias.

INTRODUCTION

This paper describes the results obtained from four lithium-drifted silicon (Si(Li)) detectors used to measure the electron conversion ratios of bismuth-207 (Bi^{207}). These measurements were made as part of a detector calibration procedure. The detectors were originally produced at the Langley Research Center to study electron transmission through spacecraft shielding materials at the NASA Space Radiation Effects Laboratory. The superior energy resolution of these devices provided a means to obtain reliable measurements of the bismuth-207 conversion ratios (in particular, to measure directly the ratios of the K- and L-shell conversion electrons to the M-shell conversion electrons).

Internal conversion in an atomic nucleus provides information which can be used to assign angular momentum and parity quantum numbers to nuclear states and, in some cases, to construct decay schemes for nuclei (refs. 1 and 2). Internal conversion coefficients which characterize the internal conversion process have been calculated for nearly all elements for conversion from the atomic K and L shells (refs. 1, 2, and 3). Some limited calculations of M-shell conversion coefficients are available in reference 1. Experimental values for internal conversion coefficients, however, are difficult to obtain, and frequently the published values for the same conversion process show large variations and only approximate agreement with the calculations.

For the 1064-keV gamma ray of bismuth-207, the theoretical and experimental internal conversion coefficients and the electron conversion coefficients and electron conversion ratios for the K and L shells show significant disagreements. Also, there are no known calculations of the M-shell internal conversion coefficients or measurements of the conversion ratios for K-, L-, and M-shell electrons. The purpose of this paper is to obtain reliable measurements of the ratios K/M, K/L, L/M, and K/(L + M). Reported herein are results on the measurements of the electron conversion ratios for the K, L, and M shells for the 1064-keV gamma ray. The conversion electrons were detected by lithium-drifted silicon detectors. The detector-amplifier system had sufficient resolution to obtain approximately a 10:1 peak-to-valley ratio between the L- and M-shell electron lines, which permitted an accurate determination of the electron conversion ratios.

SYMBOLS

A	amplitude of Gaussian distribution
$\hat{A}$	estimated value of A
$\overline{B}$	average number of counts per channel (app. E)
d	detector thickness
E_B	binding energy of electron to nucleus
E_{compt}	energy of Compton scattering event
ΔE	energy difference between two excited nuclear levels
E^e	electron energy

E^p photon energy

E^s energy of summed event

E^x X-ray energy

E^e_K, E^e_L, E^e_M K-, L-, and M-shell electron energies, respectively

E^x_i (i=1,2,3,4) X-ray energies defined in appendix A

e base of natural system of logarithms, 2.71828

F function

h precision index of Gaussian distribution $\left(h^2 = 2\sigma^2\right)$

$\hat{h}$ estimated value of h

ΔI scalar change in nuclear angular momentum

K,L,M K-, L-, and M-shell atomic electrons, respectively (when used in ratios, these symbols represent N_K, N_L, and N_M, respectively)

$(L/M)_{RD}$ ratio of backscattered electrons as calculated from raw data

m_j, β_j constants

N_{compt} number of Compton events

N_L, N_K, N_M number of K-, L-, and M-shell electrons, respectively

$N_{K,c}, N_{L,c}, N_{M,c}$ number of K-, L-, and M-shell electrons calculated from normal curves fitted to experimental peaks

$N_{K,I}, N_{L,I}, N_{M,I}$ number of K-, L-, and M-shell electrons incident on Si(Li) detector

$N_{K,o}, N_{L,o}, N_{M,o}$ number of K-, L-, and M-shell electrons observed

N_Γ number of 1770-keV gamma rays

n number of channels over which summation is performed in appendix D

p constant (percentage of electrons that backscatter)

r classical electron radius

$S_{K2}, S_{K3}, S_{L2}, S_{K4}$ number of summed events with energy corresponding to $E_K^e + E_2^x$, $E_K^e + E_3^x$, $E_L^e + E_2^x$, and $E_K^e + E_4^x$, respectively

T_K, T_L, T_M number of counts in K-, L-, and M-shell conversion electron lines, respectively, with the assumption that there were no summed events

X_i (i=1,2,3,4) number of X-rays of energy E_i^x (i = 1, 2, 3, 4) passing through detector volume during a particular run

$x_{i,c}$ calculated channel number of pulse-height distribution (i = 1, 2, . . . 400)

$x_{i,o}$ observed channel number (i = 1, 2, . . . 400)

$y_{i,c}$ calculated number of counts per channel (i = 1, 2, . . . 400)

$y_{i,o}$ observed number of counts per channel (i = 1, 2, . . . 400)

$\alpha_K, \alpha_L, \alpha_M$ K-, L-, and M-shell electron conversion coefficients

$\alpha_1 KL_{III}, \alpha_2 KL_{II}, \beta_1 KM_{III}$ X-ray notation for transitions between electronic shells and subshells

ϵ_i (i=1,2,3,4) detection efficiency for X-rays of energy E_i^x (i = 1, 2, 3, 4)

η slope of a straight line

θ_i amplitude of input analog pulse (i = 1, 2, . . . 400)

κ constant

μ mass (or linear) attenuation coefficient (subscripts 2, 3, and 4 denote association with energy ranges E_2^x, E_3^x, and E_4^x, respectively); mean channel or peak centroid

$\hat{\mu}$ estimated mean channel

$$\rho = \frac{E^p}{511 \text{ keV}}$$

σ standard deviation for Gaussian distribution

e^{σ} average collision cross section

$$\chi^2 = \sum_{i=1}^{400} \frac{(y_{i,o} - y_{i,c})^2}{y_{i,c}}$$

$$\varphi = \sum_{i=1}^{400} (x_{i,o} - x_{i,c})^2$$

Ω solid angle subtended by source at detector

ABBREVIATIONS

ADC analog-to-digital converter

FET field effect transistor

FWHM full width at half maximum of peak in pulse-height distribution

APPARATUS AND PROCEDURE

Detector Response

Figure 1 shows the response of a 3-mm Si(Li) detector to the gamma rays, X-rays, and conversion electrons from bismuth-207. This isotope emits a group of low-energy X-rays, three gamma rays, and the conversion electrons associated with each gamma ray. The X-rays are efficiently absorbed by the detector and produce a sharp peak in the spectrum. The three gamma rays are sufficiently energetic to interact with the detector, primarily by Compton scattering from atomic electrons in the detector volume. These interactions produce the Compton edges which are clearly evident in the figure. The monoenergetic conversion electrons associated with each gamma ray occur

immediately to the right of the Compton edge of the gamma ray. These electrons are detected with unit probability by the Si(Li) detector. The two small peaks designated as "conversion electron summed events" arise from the simultaneous absorption in the detector of an X-ray and a conversion electron. These events are further discussed in appendix A.

The spectrum in figure 1 was obtained with a spectrometer system resolution of 15 keV measured at full width at half maximum (FWHM) on the 974-keV electron line. By using the same experimental conditions but a different Si(Li) detector, the a-b portion of the spectrum in figure 1 was resolved into four lines (K, L, M, and sum lines) as shown in figure 2. The energy resolution of the detection system used to obtain this spectrum was 4 keV (FWHM) on the 974-keV electron line. The "pulser" is not related to the bismuth source and is discussed subsequently. The sum line arises from the simultaneous absorption in the detector of a 974-keV conversion electron and an X-ray of approximately 12 keV. The centroids of the L- and M-shell electron lines differ in energy by 12 keV and were not resolved by the spectrometer used for figure 1. The higher resolution system used in figure 2 was able to separate these lines with a peak-to-valley ratio of approximately 10:1. The four Si(Li) detectors and amplifying system used in this investigation gave a total-system resolution between 4 and 5 keV (FWHM) for all measurements.

The bismuth-207 isotope (see decay scheme in fig. 3) is primarily a gamma-ray emitter with the most intense gamma ray arising from the 1064-keV M4 transition. (An M4 transition is one for which the selection rule is $\Delta I = 4$, yes.) However the nucleus can also eject atomic electrons from the atom through an alternate process known as electron conversion. The atomic electrons in the K, L, M, . . . shells have a finite probability of penetrating the nuclear matter. Those electrons which have orbits nearest the nucleus spend, on the average, a larger fraction of their time within the nucleus. During that time the nucleus can decay from an excited state to a state of lower energy by converting the energy difference between the two states into kinetic energy of the atomic electron, which is then ejected from the atom. If the energy difference between two excited nuclear levels is denoted by ΔE and the binding energy of the electron to the nucleus is E_B, then the observed kinetic energy of the ejected electron is given by

$$E^e = \Delta E - E_B$$

Since the energy difference between excited nuclear levels is a constant and the electron binding energy is also a constant, the ejected electrons are monoenergetic.

EXPERIMENTAL CONDITIONS

A bare, isotopically pure Bi^{207} source deposited on a thin-plastic film was used for all measurements. The source strength was approximately 1 μCi (1 curie = 3.70×10^{10} disintegrations per second), and the source area was approximately 3 mm^2.

Details of the experimental apparatus are given in appendix B. In brief, the detector-amplifier system and multichannel analyzer were set to view an energy range from approximately 940 keV to 1070 keV. Energy resolution was approximately 0.4 keV per channel. All measurements reported herein were made with the detectors cooled to liquid nitrogen temperature (77 K) and at a pressure of less than 5×10^{-7} torr (1 torr = 133.322 N/m^2). The leakage current in the detectors was nominally 10^{-9} ampere at 500 volts bias. The capacitance of the detectors was between 9 pF and 15 pF. Electronic noise in the detection system varied between 3 and 4 keV (FWHM) as determined by the precision-pulse generator, and the resolution of the total system for the four detectors varied between 4 and 5 keV (FWHM) for the 974-keV K-shell conversion electrons. Figure 2 shows a typical spectrum for the conversion electrons associated with the 1064-keV gamma ray. It should be noted that the channel-number scale for figure 2 has been corrected for system nonlinearity (see app. C).

DATA ANALYSIS

A computer program was written to analyze pulse-height spectra such as the one shown in figure 2. The program first corrected each distribution for nonlinearity in the analog-to-digital conversion process (app. C). The program calculated the best-fit Gaussian curve (app. D) for each of the five peaks in each spectrum and corrected the integrated number of counts in each peak for summed events between conversion electrons and X-rays (app. A). In appendixes C and D, $x_{i,o}$ designates the ith channel in the observed pulse-height distribution and is used as an integer variable with values from 1 to 400. The subscript i also denotes the ith channel, and $i = 1, 2, \ldots 400$. Thus, for observed channel 197, for example, $x_{i,o} = x_{197,o} = 197$. The symbol $x_{i,c}$ represents a calculated value for the ith channel and is used as a real variable; for example, $x_{i,c} = x_{197,c} = 197.85$.

Distortions to the electron conversion spectra caused by electrons backscattered from the Si(Li) detectors were also taken into account (app. E). Compton scattering events in the detectors from the 1770-keV gamma ray were negligible (app. F). From the corrected integrated number of counts, the electron conversion ratios were obtained for each spectrum. In figure 4, all ratios from the data for all detectors are shown.

RESULTS AND DISCUSSION

Sixty-one spectra of the conversion electrons from the 1064-keV gamma ray of Bi^{207} were accumulated by using four similar Si(Li) detectors. The combined results of all calculations of the conversion electron ratios are given in table I. The final value of each of the ratios K/L, K/M, K/(L + M), and L/M is a weighted average of the values obtained from all measurements on all detectors. Values in parentheses are the standard deviations of the measurements.

In table II the present values of the electron conversion ratios are presented together with previously published theoretical and experimental values. The theoretical values quoted were derived from the tables of internal conversion coefficients in references 1, 2, and 3. It was assumed that the 1064-keV gamma ray of Bi^{207} resulted from an M4 transition. Values of the internal conversion coefficients for each atomic shell were plotted on log-log paper as functions of gamma-ray energy. In reference 1 conversion coefficients are given for the K, L, and M electron shells, and thus all four conversion ratios listed in table II can be calculated. In reference 2 the coefficients for K and L electron shells are given which permit only a value for the ratio K/L to be calculated. In reference 3, in addition to the K- and L-shell conversion coefficients, the M-shell conversion coefficients are given for gamma-ray energies up to 500 keV. In figure 5 a value for the total conversion coefficient for the M shell was obtained by extrapolating the theoretical data of reference 3 to 1064 keV. The extrapolated value (3.7×10^{-3}) is subject to large uncertainty. The values from reference 3, shown in figure 5, all lie below those of reference 1. The arbitrary assumption was made that the extrapolated data of reference 3 have the same curvature as the interpolated data of reference 1. This assumption gives a value of 7×10^{-3} for the coefficient and a value of 15 for the ratio K/M. The experimental values for the electron conversion ratios in table II are quoted as given in references 4, 5, and 6 except for the values of K/M and L/M given for reference 4, which were calculated from the values of K/L and K/(L + M) in that reference.

It is evident from table II that there is both a significant lack of experimental and theoretical results and a wide variation among the results that do exist. Table II shows that the present values for the ratio K/(L + M) are lower (by 3.7 to 2.4 percent) than previously reported experimental values. The ratio K/L reported herein is higher by 7.1 percent and the ratios K/M and L/M are 43 and 46 percent lower, respectively, than the only previously reported measurements of these ratios. The reason for the differences between the ratios reported herein and the previously reported work is not known. However, the four SI(Li) detectors used in this investigation yield consistent values for the conversion ratios. Only an approximate comparison can be made between

the present results and the theoretical values of conversion electron ratios extrapolated from the latest tables of internal conversion coefficients (ref. 3). A better comparison between the present data and theoretical calculations cannot be obtained until M-shell electron conversion coefficients are calculated for photon energies greater than 500 keV.

CONCLUDING REMARKS

The electron conversion ratios for the 1064-keV gamma ray of bismuth-207 have been measured by using lithium-drifted silicon (Si(Li)) detectors. Sixty-one determinations of each ratio were made with four detectors with a system resolution between 4 and 5 keV for the 974-keV conversion electrons. The data were corrected to account for summed events between conversion electrons and X-rays, Compton events in the spectra, electron backscatter from the detectors, and nonlinearity in the analog-to-digital conversion process.

The results from the four Si(Li) detectors gave the weighted average values $\frac{K}{L} = 3.90\ (\pm 0.03)$, $\frac{K}{M} = 11.23\ (\pm 0.22)$, $\frac{K}{L + M} = 2.90\ (\pm 0.03)$, and $\frac{L}{M} = 2.89\ (\pm 0.05)$. Uncertainties are statistical. The present values for the ratio $K/(L + M)$ are lower (by 3.7 to 24 percent) than previously reported experimental values. The ratio K/L reported herein is higher by 7.1 percent and the ratios K/M and L/M are 43 and 46 percent lower, respectively, than the only previously reported measurements of these ratios. The reason for the differences between the ratios reported herein and the previously reported work is not known. However, the four Si(Li) detectors used in this investigation yield consistent values for the conversion ratios.

Only an approximate comparison can be made between the values reported herein and conversion electron ratios extrapolated from the latest tables of internal conversion coefficients. A better comparison between the present data and theoretical calculations cannot be obtained until M-shell electron conversion coefficients are calculated for photon energies greater than 500 keV.

Langley Research Center,
National Aeronautics and Space Administration,
Hampton, Va., August 10, 1970.

APPENDIX A

CORRECTION FOR SUMMED EVENTS BETWEEN X-RAYS AND CONVERSION ELECTRONS

When an orbital electron is ejected from the atom in the electron conversion process, the atom is left in an excited state. The remaining electrons undergo a rapid rearrangement to reach the equilibrium or lowest energy state of the normal atom. In this deexcitation process, a series of X-rays are emitted which are characteristic of the atom. These X-rays appear almost simultaneously with the converted electron and have a finite probability of interacting with the Si(Li) detector. If an electron of energy E^e and an X-ray of energy E^x deposit all their energy in the Si(Li) detector, then the output is a summed event of energy E^s given by

$$E^s = E^e + E^x$$

The number and energy of such summed events must be determined to properly correct the observed conversion electron ratios.

Bismuth-207 decays by electron capture to an excited state of lead-207 (Pb^{207}), which in turn decays to the ground state through gamma-ray emission or internal conversion. If the lead-207 nucleus decays by internal conversion, then X-ray emission will follow. Since neither gamma-ray emission nor internal conversion involves any change in the nuclear charge, the X-ray spectrum is characteristic of the lead-207.

From the X-ray wavelengths for lead-207 presented in reference 7, it is noted that the X-rays fall into the following four separate energy ranges: 0.1189 to 3.202 keV, 9.1845 to 15.843 keV, 72.8042 to 74.9694 keV, and 84.450 to 88.06 keV. If these X-ray energy ranges are denoted E_1^x, E_2^x, E_3^x, and E_4^x, respectively, then it is possible to have summed events between X-rays of these energies and the monoenergetic conversion as follows:

$$E_K^e + E_1^x = E_K^e$$

$$E_K^e + E_2^x = E^s$$

$$E_K^e + E_3^x = E_L^e$$

$$E_K^e + E_4^x = E_M^e$$

$$E_L^e + E_2^x = E_M^e$$

$$E_M^e + E_1^x = E_M^e$$

$$E_L^e + E_1^x = E_L^e$$

APPENDIX A

The possible X-rays are grouped into the four energy ranges for two reasons: (1) There is only one summed peak observed in the spectrum which corresponds to an energy $E_K^e + E_2^x$; and (2) the finite resolution of the detection system did not permit observation of a particular X-ray and particular conversion electron.

Although the previously mentioned summed events are possible, the detection efficiency varies with the energy of the photons and detector thickness. The detection efficiency for electrons of Si(Li) detectors is 100 percent. For the purposes of this analysis, it is assumed that the X-ray detection efficiency ϵ is proportional to $e^{-\mu d}$ where μ is the mass attenuation coefficient and d is the detector thickness. It is also assumed that the conversion electrons and X-rays are emitted isotropically and that the probability of an electron and X-ray being simultaneously incident on the sensitive volume of the Si(Li) detector is given by Ω, the solid angle subtended by the source at the detector.

In order to calculate the corrections to spectra for summed events, the following definitions are used:

ϵ_i (i=1,2,3,4) — detection efficiency for X-rays of energy E_i^x (i = 1, 2, 3, 4)

$N_{K,o}, N_{L,o}, N_{M,o}$ — number of K-, L-, and M-shell conversion electrons observed

X_i (i=1,2,3,4) — number of X-rays of energy E_i^x (i = 1, 2, 3, 4) passing through detector active volume during a particular run

$S_{K2}, S_{K3}, S_{L2}, S_{K4}$ — number of summed events with energy corresponding to $E_K^e + E_2^x$, $E_K^e + E_3^x$, $E_L^e + E_2^x$, and $E_K^e + E_4^x$, respectively

T_K, T_L, T_M — number of counts in K-, L-, and M-shell conversion electron lines, respectively, with the assumption that there were no summed events

With these definitions, it is desired to determine the values of T_K, T_L, and T_M from the observed spectra. Since each summed event either removes one count from a conversion electron line or adds one to it, the equations for the number of electrons observed in each line are

$$\left.\begin{aligned} N_{K,o} &= T_K - S_{K2} - S_{K3} - S_{K4} \\ N_{L,o} &= T_L + S_{K3} - S_{L2} \\ N_{M,o} &= T_M + S_{L2} + S_{K4} \end{aligned}\right\} \qquad \text{(A1)}$$

where the expressions for the number of summed events are given by

$$\left.\begin{aligned} S_{K2} &= \Omega\epsilon_2 X_2^K \\ S_{K3} &= \Omega\epsilon_s X_3 \\ S_{K4} &= \Omega\epsilon_4 X_4 \\ S_{L2} &= \Omega\epsilon_2 X_2^L \end{aligned}\right\} \tag{A2}$$

The superscripts K and L on X_2 denote electron conversion from the K and L shells with subsequent emission of an X-ray of energy E_2^x. By using expressions (A2) in equations (A1) and solving for T_K, T_L, and T_M, the following results are obtained:

$$\left.\begin{aligned} T_K &= N_{K,o} + \Omega\left(\epsilon_2 X_2^K + \epsilon_3 X_3 + \epsilon_4 X_4\right) \\ T_L &= N_{L,o} - \Omega\left(\epsilon_3 X_3 - \epsilon_2 X_2^L\right) \\ T_M &= N_{M,o} - \Omega\left(\epsilon_2 X_2^L + \epsilon_4 X_4\right) \end{aligned}\right\} \tag{A3}$$

In the electron conversion process when a K-shell electron is ejected from the atom, an electron from one of the other electron shells will fill the K-shell vacancy. In lead-207 there are nine possible transitions between the outer shells and the K shell, but they are not equally probable. The most likely transition is between the subshell L_{III} and the K shell. The X-ray emitted in this transition is designated (in the notation of ref. 7) as $\alpha_1 KL_{III}$; the X-rays emitted in the second and third most probable transitions are designated as $\alpha_2 KL_{II}$ and $\beta_1 KM_{III}$, respectively. The intensity ratios among these X-rays are as follows:

$$\alpha_1 KL_{III}:\alpha_2 KL_{II}:\beta_1 KM_{III} = 100:50:18$$

The $\alpha_1 KL_{III}$ and $\alpha_2 KL_{II}$ X-rays have energies in the E_3^x range, and the energy of the $\beta_1 KM_{III}$ X-ray lies in the E_4^x range. By using the intensity ratios, the number of X-rays of energy E_3^x passing through the detector is given by

$$X_3 = \frac{150}{168} T_K$$

and the number of X-rays of energy E_4^x is given by

$$X_4 = \frac{18}{168} T_K$$

APPENDIX A

It is assumed that for each transition between the L and K shells, there is a transition from either the M or N shell to the L shell which produces an X-ray in the E_2^x range. The number of such X-rays is then given by

$$X_2^K = X_3 = \frac{150}{168} T_K$$

where superscript K denotes electron conversion from the K shell. It is also assumed that for each L-shell electron ejected from the atom, one X-ray of energy E_2^x is emitted. The number of such X-rays is simply

$$X_2^L = T_L$$

where superscript L denotes electron conversion from the L shell.

The solid angle Ω in equations (A3) depends on the cross-sectional area of the sensitive region of the detector and the source-to-detector distance (which was a constant in all measurements). A value of Ω for each detector can be obtained from the expression

$$\Omega = \frac{S_{K2}}{\epsilon_2 X_2^K} = \frac{S_{K2}}{\frac{150}{168}\epsilon_2 T_K}$$

By using the preceding information, equations (A3) become

$$T_K = N_{K,o} + S_{K2}\left(1 + \frac{\epsilon_3}{\epsilon_2} + \frac{18}{150}\frac{\epsilon_4}{\epsilon_2}\right)$$

$$T_L = \left(N_{L,o} - \frac{\epsilon_3}{\epsilon_2} S_{K2}\right) \Bigg/ \left(1 - \frac{168}{150}\frac{S_{K2}}{T_K}\right)$$

and

$$T_M = N_{M,o} - S_{K2}\left(\frac{168 T_L}{150 T_K} + \frac{18}{150}\frac{\epsilon_4}{\epsilon_2}\right)$$

Next, the detection efficiency is considered. For X-rays with energies in the range E_2^x and a detector thickness of 0.3 cm, the probability of interaction is given by

$$\epsilon_2 = 1 - e^{-\mu_2 d} = 1 - e^{-14.52} \approx 1$$

For X-rays with energies of E_3^x, the interaction probability is

$$\epsilon_3 = 1 - e^{-\mu_3 d} = 1 - e^{-0.158} \approx 0.15$$

and for X-rays with energies of E_4^x,

$$\epsilon_4 = 1 - e^{-\mu_4 d} = 1 - e^{-0.138} \approx 0.13$$

With these values used for ϵ_i,

$$T_K = N_{K,0} + 1.1656 S_{K2}$$

$$T_L = \left(N_{L,o} - 0.15 S_{K2}\right) \Big/ \left(1 - 1.12 \frac{S_{K2}}{T_K}\right)$$

and

$$T_M = N_{M,o} - S_{K2}\left(1.12 \frac{T_L}{T_K} + 0.016\right)$$

The values of $N_{K,o}$, $N_{L,o}$, and $N_{M,o}$ are independent of geometrical factors. They depend only on the observed spectra and the mass attenuation coefficients for the X-ray.

The values for T_K, T_L, and T_M obtained from these equations are used to determine the electron conversion ratios; that is,

$$\frac{K}{L} = \frac{T_K}{T_L}$$

$$\frac{K}{L + M} = \frac{T_K}{T_L + T_M}$$

$$\frac{L}{M} = \frac{T_L}{T_M}$$

and

$$\frac{K}{M} = \frac{T_K}{T_M}$$

In these expressions summed events between conversion electrons from the 590-keV and 1064-keV gamma rays have been neglected since the number of counts in the sum lines (see fig. 1) is less than 0.2 percent of the integrated number of counts in the 974-keV conversion electron line.

Summed events which arise from the simultaneous absorption of a conversion electron and an Auger electron in a Si(Li) detector have not been considered in this discussion. In reference 8 the calculated energies of KLL Auger electrons are given for lead-207. The minimum and maximum energies of this group are 55.96 keV and 61.658 keV, respectively. Thus, any summed events between K-shell conversion

electrons and KLL Auger electrons would have an energy range from approximately 1030 keV to 1036 keV, and these events would appear in figure 2 between channel numbers of approximately 290 and 320. At most, such events would be an order of magnitude less than the summed events between X-rays and conversion electrons.

APPENDIX B

EXPERIMENTAL APPARATUS

The four Si(Li) detectors used in the measurements reported herein were fabricated by using techniques developed at the Langley Research Center. The detectors were made from 10 kΩ-cm, p-type, boron-doped, float-zoned purified silicon wafers, 3 mm thick and 1.8 cm in diameter. Figure 6 shows a cross section of a typical detector and a list of characteristics. Additional information on these detectors and their use as low-energy photon spectrometers can be found in reference 9.

The electronic system used to determine the detector energy resolution is shown in figure 7. High voltage from a bias supply was fed to the detector through a 2000-MΩ load resistor in a field-effect-transistor (FET) preamplifier. Signals from the preamplifier were fed to the main amplifier for further amplification and pulse shaping. The best time constants were found to be 0.8 μs for the first differentiation and 0.8 μs for the integration time. The second differentiator was set at 1 ms. The bipolar pulses from the main amplifier were then fed to a bias amplifier to further amplify a selected portion of the pulse-height spectrum; the pulses from the bias amplifier were, in turn, fed directly to the analog-to-digital converter circuits of a 400-channel, pulse-height analyzer. The total gain of the system was adjusted to give an energy-per-channel resolution of approximately 0.4 keV. A precision-pulse generator was connected to the preamplifier and adjusted to position the pulser between the K- and L-shell conversion electron lines from the Bi^{207} calibration course in the pulse-height spectrum. The width of the pulser indicated the electrical noise of the amplifying system. To minimize spectrum distortions due to any changes in the amplifier system gain, the pulser was used as a reference point for a pulse-height spectrum stabilizer, which corrected for any gain shifts in the system. The stabilizer could hold the system gain constant to ±1 channel.

Figure 8 shows an overall view of the arrangement used in measuring the electron conversion ratios. The small vacuum chamber containing the Bi^{207} source and detector was connected to a larger chamber through a gate valve. The large chamber was maintained at a pressure below 2.66×10^{-6} N-m^2 for all tests reported herein. No oil film was observed on the detectors at this pressure for periods of up to 1 week. The detector holder was attached to the end of a copper-rod cold finger inside the small chamber. The detector could be cooled from room temperature to approximately liquid nitrogen temperature in about 15 minutes by immersing the copper rod in a reservoir of liquid nitrogen. Some detectors were cycled from 295 K to 77 K and back to 295 K as many as five times in a 15-hour period without any apparent damage. The detector was connected to an external preamplifier via an electrical connector in the wall of the small chamber.

APPENDIX C

CORRECTION FOR SYSTEM NONLINEARITY

A relatively large integral nonlinearity was discovered in the electronic system during the analysis of the data. The nonlinearity was measured, and the final data were corrected to remove the effects of the nonlinearity.

There is, in an ideal analog-to-digital converter (ADC) system, a linear relationship between the amplitude of the input analog pulse and the digital output. Thus, to correct for the nonlinearity of a particular electronic system, the actual relationship between input pulse and digital output must be measured. From this information it is possible to determine the corrections to the digital output such that the final output data depend linearly on the input analog pulse.

A precision-pulse generator was used to simulate the output pulses from the Si(Li) detectors, and all instrument settings and physical conditions were maintained exactly the same as for the detector tests. The dependence of channel location on input-pulse amplitude was obtained in graphic form as shown in figure 9. The analog-to-digital conversion process was linear up to approximately channel number 185.

If θ_i represents the amplitude of the input analog pulse and $x_{i,c}$ represents the corresponding channel number, then for a linear system,

$$\theta_i = \eta x_{i,c} + \kappa \tag{C1}$$

where η is the slope of the straight line and κ is a constant. For a nonlinear system it is assumed that there exists a function $F(x_{i,o})$ which relates the input-pulse amplitude θ_i to an observed channel number $x_{i,o}$; that is,

$$\theta_i = F(x_{i,o}) \tag{C2}$$

For a given amplitude θ_i, equations (C1) and (C2) give

$$\theta_i = \eta x_{i,c} + \kappa = F(x_{i,o}) \tag{C3}$$

By solving for $x_{i,c}$ the following result is obtained:

$$x_{i,c} = \frac{F(x_{i,o}) - \kappa}{\eta} \tag{C4}$$

This expression converts the observed channel number from the nonlinear system to a channel number in the linear system, provided $F(x_{i,o})$, η, and κ are known.

The ADC system was found to be linear from channels 50 to 185. The desired linear system parameters κ and η were chosen to be the same as those in the linear

response range of the actual ADC system (channels 50 to 185). The data of figure 9 were replotted on semilog paper, and it was observed that the data could be approximated by a series of five straight lines. Thus, $F(x_{i,o})$ could be represented sectionally as

$$F_j(x_{i,o}) = \beta_j e^{m_j x_{i,o}} \qquad (j = 1, 2, \ldots 5) \qquad \text{(C5)}$$

between channels 185 and 370. The parameters β_j and m_j for each of the five sectional functions of the form of equation (C5) were found by fitting the best straight lines to the data. Values of $x_{i,c}$ from equation (C4) matched the experimental points to within ± 1.0 channel.

APPENDIX D

GAUSSIAN CURVE-FITTING METHOD

In analyzing the response of Si(Li) detectors to either low-energy electromagnetic radiation or charged particles, the basic assumption that is normally made is that the results can be well approximated by a Gaussian or normal curve of the form

$$y_{i,c} = Ae^{-\left(\frac{x_{i,o}-\mu}{h}\right)^2} \tag{D1}$$

where $y_{i,c}$ represents the calculated number of counts per channel and $x_{i,o}$ is the observed channel number of the pulse-height distribution. The curve parameters A, μ, and h correspond, respectively, to the amplitude, mean channel or peak centroid, and precision index. The precision index is related to the standard deviation σ by

$$h^2 = 2\sigma^2 \tag{D2}$$

The problem is to find a set of values for (A,μ,h) which gives the best fit to the data where, in general, the best fit is determined by the minimum of the sum of squares of the deviations between the observed data and calculated values $\left(\text{that is, the minimum } \sum_{i=1}^{400}\left(y_{i,o} - y_{i,c}\right)^2\right)$. The mathematical form of the normal distribution, however, does not permit simple expressions for the parameters in terms of the dependent and independent variables when the usual least-squares criterion is used. The procedure used to determine the best normal curve to fit the data is relatively simple although perhaps not as accurate as other more complex computer programs for curve fitting.

The approach taken is to interchange the role of the dependent and independent variables in equation (D1); that is

$$y_{i,o} = Ae^{-\left(\frac{x_{i,c}-\mu}{h}\right)^2} \tag{D3}$$

By taking the natural logarithm of both sides of equation (D3) and solving for $x_{i,c}$, the result is

$$x_{i,c} = \mu \pm h\left(\ln A - \ln y_{i,o}\right)^{1/2} \tag{D4}$$

In this expression the independent variable is defined to be $y_{i,o}$, the observed number of counts per channel. For a given set of parameter values and a value for $y_{i,o}$, a channel number $x_{i,c}$ can be determined which, for a good curve fit, should have nearly the same

value as the observed channel number $x_{i,o}$. Under the assumption that the best curve fit minimizes the deviations between observed and calculated channel numbers, it is desired to minimize a function φ, defined as

$$\varphi = \sum_{i=1}^{400} (x_{i,o} - x_{i,c})^2 \tag{D5}$$

where $x_{i,o}$ represents the observed channel number and $x_{i,c}$ is the calculated channel number. With the use of equation (D4) the expression for φ in equation (D5) becomes

$$\varphi = \sum_{i=1}^{400} \left\{ x_{i,o} - \left[\mu \pm h\left(\ln A - \ln y_{i,o}\right)^{1/2} \right] \right\}^2$$

By expanding the squared term and carrying out the indicated summation over n channels, the following equation is obtained:

$$\varphi = \sum_{i=1}^{400} x_{i,o}^2 - 2\mu \sum_{i=1}^{400} x_{i,o} + n\mu^2 + h^2 n \ln A \mp 2h \sum_{i=1}^{400} \left[x_{i,o}\left(\ln A - \ln y_{i,o}\right)^{1/2} \right]$$

$$\pm 2\mu h \sum_{i=1}^{400} \left(\ln A - \ln y_{i,o}\right)^{1/2} - h^2 \sum_{i=1}^{400} \ln y_{i,o} \tag{D6}$$

Then φ is minimized with respect to the mean channel μ by

$$\frac{\partial \varphi}{\partial \mu} = 0 \tag{D7}$$

which yields the expression

$$\mu = \frac{\sum_{i=1}^{400} x_{i,o} \mp h \sum_{i=1}^{400} \left(\ln A - \ln y_{i,o}\right)^{1/2}}{n} \tag{D8}$$

Next φ is minimized with respect to the precision index h by

$$\frac{\partial \varphi}{\partial h} = 0$$

which gives

$$h = \frac{\pm n \sum_{i=1}^{400} \left[x_{i,o} \left(\ln A - \ln y_{i,o} \right)^{1/2} \right] \mp \sum_{i=1}^{400} x_{i,o} \sum_{i=1}^{400} \left(\ln A - \ln y_{i,o} \right)^{1/2}}{n^2 \ln A - n \sum_{i=1}^{400} \ln y_{i,o} - \left[\sum_{i=1}^{400} \left(\ln A - \ln y_{i,o} \right)^{1/2} \right]^2} \tag{D9}$$

The precision index h is now a function of the amplitude A only. Furthermore, by replacing h in equation (D8) with equation (D9), it is seen that the mean channel is also a function of the amplitude only. In principle, at least, the problem has been reduced to one with only A as a variable.

In equations (D8) and (D9), the absolute value of the argument in the square-root term must be used to handle the possible case where a particular $y_{i,o}$ is greater than the amplitude A. If

$$\left(\ln A - \ln y_{i,o} \right)^{1/2} \rightarrow \left(\left| \ln A - \ln y_{i,o} \right| \right)^{1/2} \tag{D10}$$

then equations (D8) and (D9) become

$$\mu = \frac{\sum_{i=1}^{400} x_{i,o} - h \sum_{i=1}^{400} \left(\left| \ln A - \ln y_{i,o} \right| \right)^{1/2}}{n} \tag{D11}$$

and

$$h = \frac{n \sum_{i=1}^{400} \left[x_{i,o} \left(\left| \ln A - \ln y_{i,o} \right| \right)^{1/2} \right] - \sum_{i=1}^{400} x_{i,o} \sum_{i=1}^{400} \left(\left| \ln A - \ln y_{i,o} \right| \right)^{1/2}}{n^2 \ln A - n \sum_{i=1}^{400} \ln y_{i,o} - \left[\sum_{i=1}^{400} \left(\left| \ln A - \ln y_{i,o} \right| \right)^{1/2} \right]^2} \tag{D12}$$

where the $(\pm)$ sign is implicit in the square-root terms.

Normally, when using the least-squares criterion, one would also obtain an expression for A by requiring

$$\frac{\partial \varphi}{\partial A} = 0$$

However, this procedure leads to a transcendental equation in terms of two of the three parameters A, μ, and h.

APPENDIX D

To make use of equations (D11) and (D12), the amplitude A of the best-fit Gaussian curve must be known approximately and a rule to determine which sign to use in the expressions must be ascertained. For data that are well approximated by a narrow Gaussian curve, the channel with the largest number of counts is approximately the value of the amplitude of the best-fit curve and, also, is approximately the mean channel or centroid of the curve. This estimated mean channel $\hat{\mu}$ is used to determine which sign to use by the following convention:

If $x_{i,o} > \hat{\mu}$: (+)

If $x_{i,o} < \hat{\mu}$: (-)

Thus, in dealing with the square-root terms, the positive sign is used for all data points to the right of the peak centroid and the negative sign is used for all points to the left.

A convenient criterion for judging the fit of a theoretical distribution to a given data set is the chi-square test

$$\chi^2 = \sum_{i=1}^{400} \frac{\left(y_{i,o} - y_{i,c}\right)^2}{y_{i,c}} \tag{D13}$$

where $y_{i,c}$ represents calculated values from the assumed distribution and $y_{i,o}$ represents the observed values. By using tables of χ^2 as a function of degrees of freedom in the data, one obtains a certain probability that the assumed distribution does or does not fit the observed data (for a discussion of the chi-square test, see ref. 10).

In curve fitting for pulse-height spectra, the number of degrees of freedom is taken to be equal the number of data points (or channels) used in the curve fitting process less the number of parameters used to fit the curve. A rule-of-thumb criterion for deciding on a good fit is that the value of χ^2 should be approximately equal to the number of degrees of freedom. If χ^2 is more than twice the number of degrees of freedom, then the assumed distribution does not fit the data very well.

A FORTRAN IV program was written to analyze the spectrum shown in figure 2. The computer performed the same process on each line. This process involved the following steps:

(1) The data point with the largest number of counts was taken as the first estimate for the amplitude of the best-fit Gaussian curve, and the channel number for this data point was taken as the first estimate of the peak centroid.

(2) These estimated values for amplitude and peak centroid ($\hat{A}$ and $\hat{\mu}$) are used to obtain a value for the precision index and a better value for the centroid from equations (D11) and (D12).

(3) By using the value of $\hat{A}$ obtained in step (1) and the values of $\hat{h}$ and $\hat{\mu}$ obtained in step (2), a value of χ^2 is calculated from

$$\chi^2 = \sum_{i=1}^{400} \frac{(y_{i,o} - y_{i,c})^2}{y_{i,c}} = \sum_{i=1}^{400} \frac{\left[y_{i,o} - \hat{A}e^{-\left(\frac{x_{i,o}-\hat{\mu}}{\hat{h}}\right)^2}\right]^2}{\hat{A}e^{-\left(\frac{x_{i,o}-\hat{\mu}}{\hat{h}}\right)^2}}$$

where the summation extends over the range of data points used.

(4) The estimate $\hat{A}$ is changed by a small amount and new values $\hat{\mu}$ and $\hat{h}$ are calculated from equations (D11) and (D12); these new values for $\hat{A}$, $\hat{\mu}$, and $\hat{h}$ are used to compute another value of χ^2.

(5) Steps (1) to (4) are repeated with the value of $\hat{A}$ changed each time in a direction to always decrease the value of χ^2. The cycle stops when the incremental change in $\hat{A}$ reaches a predetermined limit, which is arbitrarily set at 0.1 count.

As a check on the accuracy of this method, a theoretical spectrum, similar to figure 2, consisting of four Gaussian curves, each with different values for the set of parameters (A,μ,h), was calculated; then these theoretical results were used as computer input data. The computer then determined the values $(\hat{A},\hat{\mu},\hat{h})$ that gave the best fit to the input data. Table III shows the results from this spectrum. Three other test spectra were also used. For all four tests, the calculated values are close to the exact values, with the maximum error less than 1 percent.

These results indicate that this method should give excellent Gaussian curve fits provided the "tails" of the experimental data are not used. This method is relatively simple and easy to program.

APPENDIX E

CORRECTION FOR ELECTRON BACKSCATTER

Electrons incident on the Si(Li) detectors can undergo large angle scattering and escape from the front face of the detector. These electrons lose only part of their kinetic energy in the active volume of the detector. Such events produce a "tail" on the low-energy side of a pulse-height distribution for a monoenergetic-electron source. The number of electrons that backscatter from the detector face is a function of the incident energy and angle and the atomic number of the detector material. However, this phenomenon has not been sufficiently studied either theoretically or experimentally to permit one to confidently correct experimental data on the basis of what is now known. Large differences exist among various experiments on the backscattering of electrons from silicon and other materials (refs. 11 and 12).

In principle, it is possible for an incident electron to lose any amount of its kinetic energy E^e in the detector from, essentially, zero to E^e. Consequently, in the pulse-height distribution for the conversion electrons from the 1064-keV gamma ray of bismuth-207, there are tails on the K-, L-, and M-shell lines that extend down to zero energy. Thus, there are counts in the K- and L-shell lines that correspond to K-shell electrons which have backscattered and left an amount of energy approximately equal to the K- or L-shell electrons. The same is true for some L-shell electrons that appear as K-shell electrons. To correct for these backscattered electrons in the calculation of the conversion ratios, the following reasoning was used. In references 11 and 12 the number of backscattered electrons was found not to vary greatly with incident energy around 1 MeV. The conversion electrons from the 1064-keV gamma ray vary in energy from 974 keV to approximately 1056 keV. The assumption is made that the percentage of K-, L-, and M-shell electrons that backscatter is a constant p. Let $N_{K,I}$, $N_{L,I}$, and $N_{M,I}$ represent the number of K-, L-, and M-shell electrons, respectively, incident on the Si(Li) detector. Also, let $N_{K,c}$, $N_{L,c}$, and $N_{M,c}$ represent the number of K-, L-, and M-shell electrons calculated from normal curves fitted to the experimental lines. The electron conversion ratios, which are independent of the backscattered fraction, are then given by

$$\frac{K}{L} = \frac{N_{K,I}}{N_{L,I}} = \frac{N_{K,c}/p}{N_{L,c}/p} = \frac{N_{K,c}}{N_{L,c}}$$

$$\frac{K}{M} = \frac{N_{K,I}}{N_{M,I}} = \frac{N_{K,c}/p}{N_{M,c}/p} = \frac{N_{K,c}}{N_{M,c}}$$

$$\frac{L}{M} = \frac{N_{L,I}}{N_{M,I}} = \frac{N_{L,c}/p}{N_{M,c}/p} = \frac{N_{L,c}}{N_{M,c}}$$

and

$$\frac{K}{L+M} = \frac{1}{\frac{L}{K} + \frac{M}{K}} = \frac{N_{K,c}}{N_{L,c} + N_{M,c}}$$

The preceding expressions are correct provided the raw experimental data are corrected for the tails before the normal curves are fitted to the pulse-height distribution. This correction was made by first fitting normal curves to the raw-data electron conversion lines for all measurements. The electron conversion ratios were calculated from these normal curves. Next, the number of counts in 11 channels which lay midway between the pulser and the L line were averaged together to obtain $\overline{B}$. The number of counts in these channels are assumed to have been produced by backscattered L- and M-shell electrons. The ratio of backscattered L-shell electrons to M-shell electrons over these 11 channels is assumed equal to the ratio calculated from the raw data $(L/M)_{RD}$. The average number of counts per channel $\overline{B}$ was divided by the raw-data ratio $(L/M)_{RD}$ to obtain the average number of counts per channel due to M-shell backscattered electrons – that is, $\overline{B}/(L/M)_{RD}$, which was then subtracted from each channel under the L line. The average number of counts per channel $\overline{B}$ was subtracted from each channel from channel zero up to and including the pulser. This correction was made to each set of raw data, and another set of normal curves was fitted to the K-, L-, and M-shell lines; values for $N_{K,c}$, $N_{L,c}$, and $N_{M,c}$ were calculated and used to find the conversion ratios. This correction produced about a 0.5-percent change in the raw-data ratios.

APPENDIX F

COMPTON SCATTERING

The 1064-keV and 1770-keV gamma rays from the Bi^{207} source can interact with the Si(Li) detector through Compton scattering with bound atomic electrons. The gamma-ray photons can, in a single collision, impart to an atomic electron any energy between 0 and the maximum energy of a recoil electron $\frac{E^p}{1 + \frac{1}{2\rho}}$ where E^p is the photon energy and ρ is a parameter given by $\frac{E^p}{511\ \text{keV}}$. For the 1064-keV gamma ray, the maximum energy of a recoil electron is 860 keV; for the 1770-keV gamma ray, the maximum recoil-electron energy is 1545 keV. The electron amplifying system and pulse-height analyzer were set to observe an energy range between 940 keV and 1070 keV, approximately. Consequently, Compton events from the 1064-keV gamma ray could not be observed. The 1770-keV gamma ray could produce Compton events which would fall within the observed energy range although the total number of such events would be small as shown by the following discussion.

An expression for the average collision cross section ${}_e\sigma$ (which represents the integrated probability, per electron, that some scattering event will occur) is obtained from reference 10. In the present notation this expression is

$$ {}_e\sigma = 2\pi r^2 \left\{ \frac{1+\rho}{\rho^2} \left[\frac{2(1+\rho)}{1+2\rho} - \frac{1}{\rho} \ln(1+2\rho) \right] + \frac{1}{2\rho} \ln(1+2\rho) - \frac{1+3\rho}{(1+2\rho)^2} \right\} $$

where $r = 2.818 \times 10^{-13}$ cm. For a gamma-ray energy of 1770 keV, $\rho = 3.46$ and ${}_e\sigma = 1.569 \times 10^{-25}$ cm^2/electron. The Compton total linear attenuation coefficient μ is obtained from the average collision cross section ${}_e\sigma$ by

$$ \mu = a\,{}_e\sigma $$

where a is the number of electrons per cm^3 in an absorber. Thus the number of Compton events N_{compt} for a number of 1770-keV gamma rays (N_Γ) incident on a silicon detector of thickness $d = 3$ mm is given by

$$ N_{compt} = N_\Gamma \left(1 - e^{-\mu d}\right) $$

or

$$ N_{compt} = 0.0325 N_\Gamma $$

APPENDIX F

The number of 1770-keV gamma rays N_Γ is approximately 0.1 times the number of 1064-keV gamma rays emitted from a Bi^{207} source. By using the observed number of conversion electrons from the 1064-keV gamma ray (see fig. 2, for example) and the theoretical electron conversion coefficients from reference 1, the number of 1770-keV gamma rays is given by

$$N_\Gamma \approx 0.1 \left. \frac{(N_{K,o} + N_{L,o} + N_{M,o})}{(\alpha_K + \alpha_L + \alpha_M)} \right|_{1064 \text{ keV}}$$

For the spectrum shown in figure 2, $N_\Gamma \approx 2000$. If it is assumed that these 2000 events are evenly distributed from the Compton edge at 1545 keV to zero energy, the number of Compton events per channel in figure 2 is less than 0.5, which is negligible.

REFERENCES

1. Rose, M. E.: Internal Conversion Coefficients. Interscience Publ., Inc., 1958.
2. Sliv, L. A.; and Band, I. M.: Tables of Internal Conversion Coefficients. Alpha-, Beta- and Gamma-Ray Spectroscopy, vol. 2, Kai Siegbahn, ed., North-Holland Pub. Co. (Amsterdam), 1965, pp. 1639-1672.
3. Hager, R. S.; and Seltzer, E. C.: Internal Conversion Tables. Part I: K-, L-, M-Shell Conversion Coefficients for Z = 30 to Z = 103 Nucl. Data, Sect. A, vol. 4, nos. 1 and 2, Feb. 1968.
4. Sen, S. K.; and Rizvi, S. I. H.: Accurate Determination of the Internal Conversion Coefficients of Cascade Gamma Rays. Nucl. Instrum. Methods, vol. 57, no. 2, Dec. 1967, pp. 227-228.
5. Chen, C. T.; and Hurley, F. W.: Recent References. Nucl. Data, Sect. B., vol. 1, no. 3, July 1966.
6. Andersen, V.; and Christensen, C. J.: Measurement of the Conversion Ratio for ^{207}Bi. Nucl. Phys., vol. A113, no. 1, May 1968, pp. 81-85.
7. Bearden, J. A.: X-Ray Wavelengths: Rev. Mod. Phys., vol. 39, no. 1, Jan. 1967, pp. 78-124.
8. Bergström, I.; and Nordling, C.: The Auger Effect. Alpha-, Beta- and Gamma-Ray Spectroscopy, vol. 2, Kai Siegbahn, ed., North-Holland Pub. Co. (Amsterdam), 1965, pp. 1523-1543.
9. Beck, Sherwin M.: Lithium-Drifted Silicon Detectors as Low-Energy Photon Spectrometers. NASA TN D-5056, 1969.
10. Evans, Robley D.: The Atomic Nucleus. McGraw-Hill Book Co., Inc., c.1955.
11. Rester, D. H.; and Rainwater, W. J., Jr.: Backscattering of 1-MeV Electrons From Silicon. Nucl. Instrum. Methods, vol. 41, no. 1, Apr. 1966, pp. 51-55.
12. Wright, Kenneth A.; and Trump, John G.: Back-Scattering of Megavolt Electrons From Thick Targets. J. Appl. Phys., vol. 33, no. 2, Feb. 1962, pp. 687-690.

TABLE I.- SUMMARY OF ELECTRON CONVERSION RATIOS

[Values in parentheses are standard deviations]

Detector	Average K/L	Average K/M	Average K/(L + M)	Average L/M
1	3.9297 (0.0543)	11.5677 (0.3840)	2.9328 (0.0465)	2.9437 (0.0891)
2	3.9188 (0.0686)	11.0841 (0.3290)	2.8945 (0.0421)	2.8294 (0.1008)
3	3.8616 (0.0621)	11.1157 (0.2661)	2.8656 (0.0419)	2.8789 (0.0736)
4	3.8893 (0.0719)	11.2696 (0.2519)	2.8913 (0.0514)	2.8978 (0.0531)
Weighted average:	3.9020	11.2289	2.8995	2.8919
Standard deviation of weighted average:	0.0308	0.224	0.0277	0.0475

TABLE II.- COMPARISON OF PRESENT EXPERIMENTAL RESULTS WITH AVAILABLE EXPERIMENTAL AND THEORETICAL VALUES

Conversion ratios	Experiment				Theory		
	Present results	Ref. 4	Ref. 5	Ref. 6	Ref. 1	Ref. 2	Ref. 3
K/L	3.90 ± 0.03	3.64 ± 0.10			2.78	3.76	3.75
K/M	11.23 ± 0.22	19.60			8.8		15.0
K/(L + M) . . .	2.90 ± 0.03	3.07 ± 0.09	3.4, 3.0, 3.8	3.37	2.11		3.0
L/M	2.89 ± 0.05	5.38			3.16		4.0

TABLE III.- ACCURACY OF GAUSSIAN CURVE-FITTING METHOD

Parameter	Test no.	Exact value	Fitted value	Difference
Amplitude	1	4 949	4 949.0	0
	2	5 333	5 333.0	0
	3	1 234	1 233.6	-.4
	4	601	599.6	-1.4
Mean channel	1	110.980	110.9799	-0.0001
	2	211.505	211.5048	-.0002
	3	310.505	310.510	.005
	4	340.905	340.865	-.040
Standard deviation	1	5.952	5.9519	-0.0001
	2	4.123	4.1229	-.0001
	3	6.321	6.3308	.0098
	4	6.678	6.7395	.0615
Integrated count	1	67 827	67 826	-1
	2	54 227	54 227	0
	3	17 659	17 658	-1
	4	8 890	8 894	4

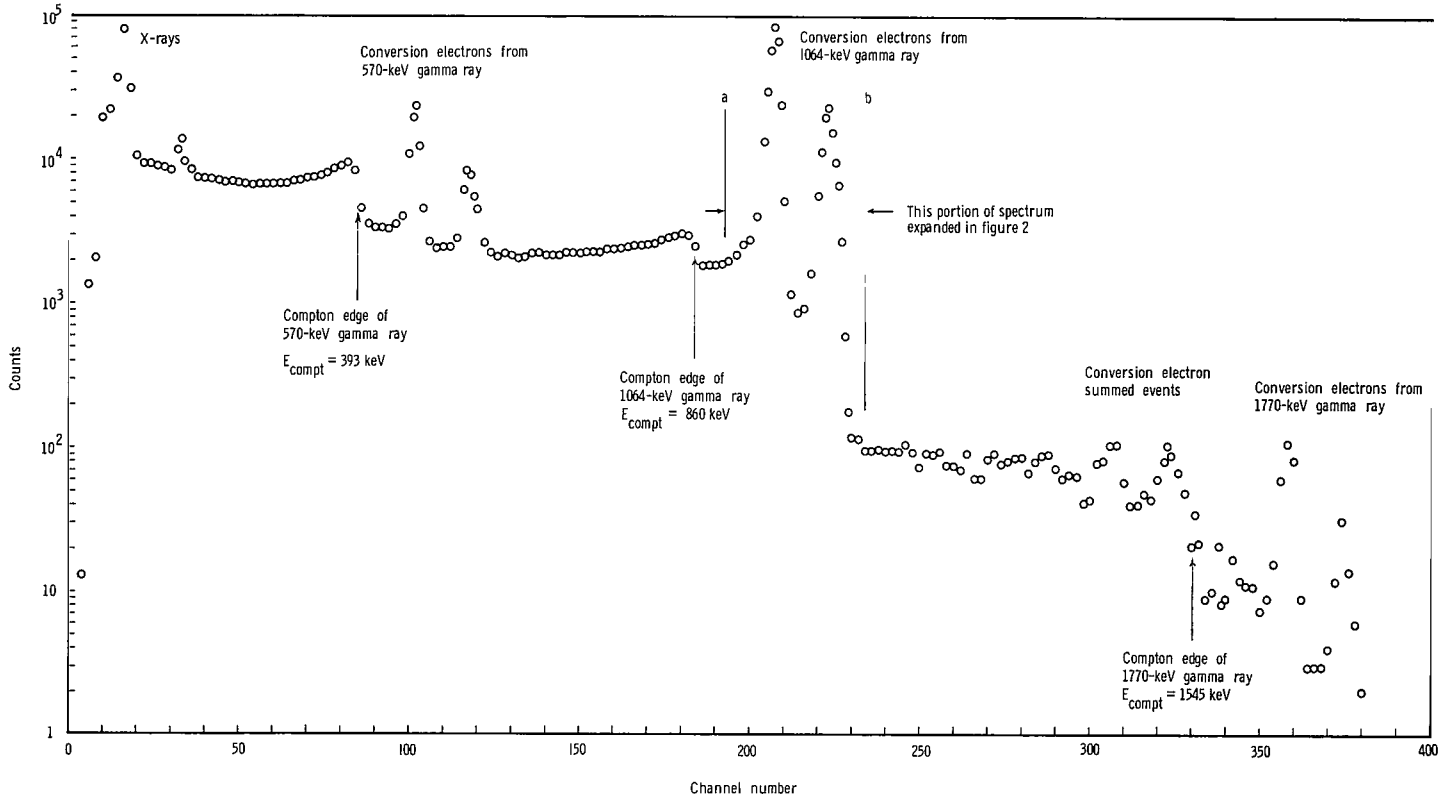

Figure 1.- Pulse-height spectrum of bismuth-207.

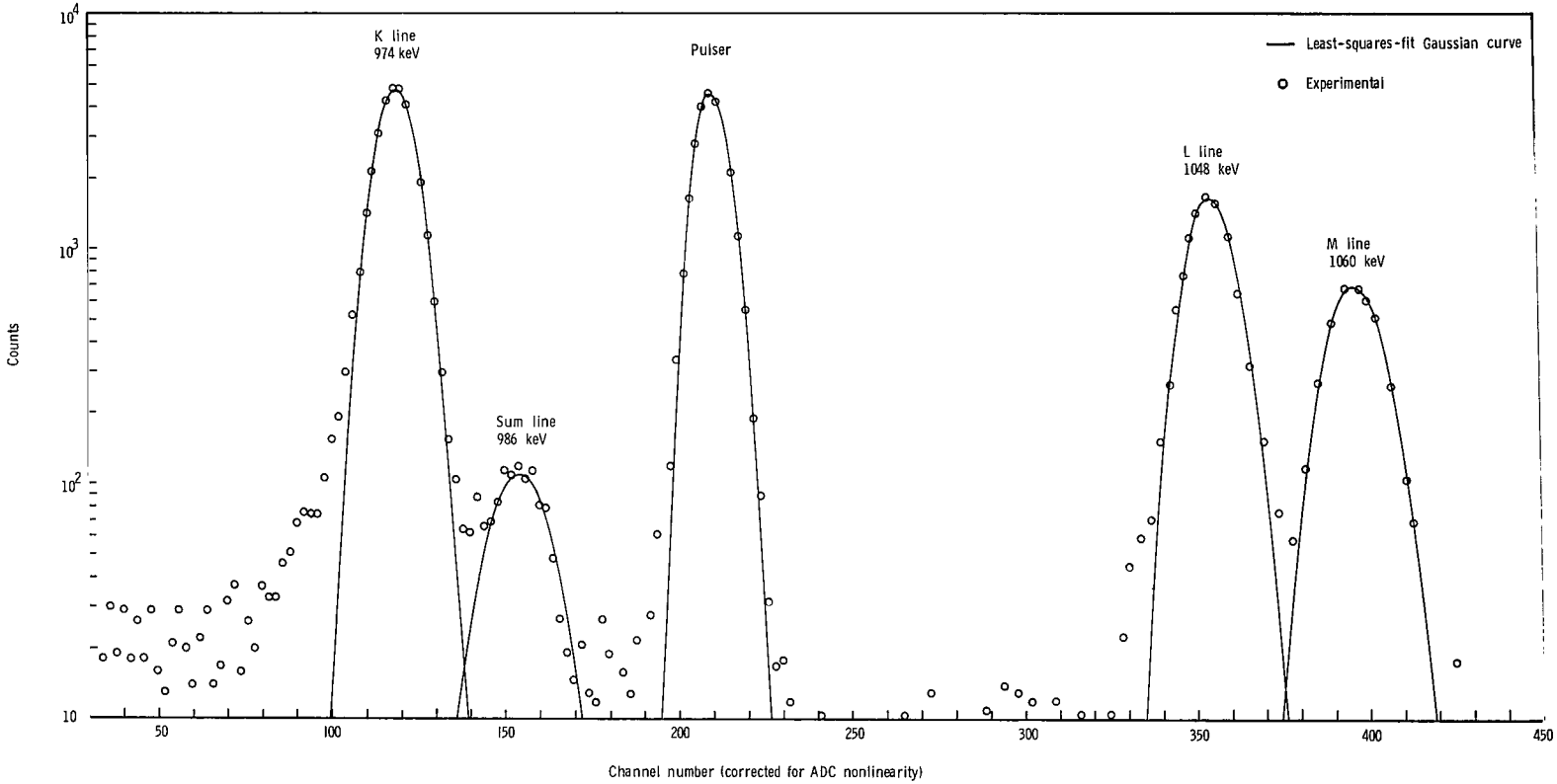

Figure 2.- Pulse-height spectrum of conversion electrons from 1064-keV gamma ray of bismuth-207 (expanded region a-b of fig. 1).

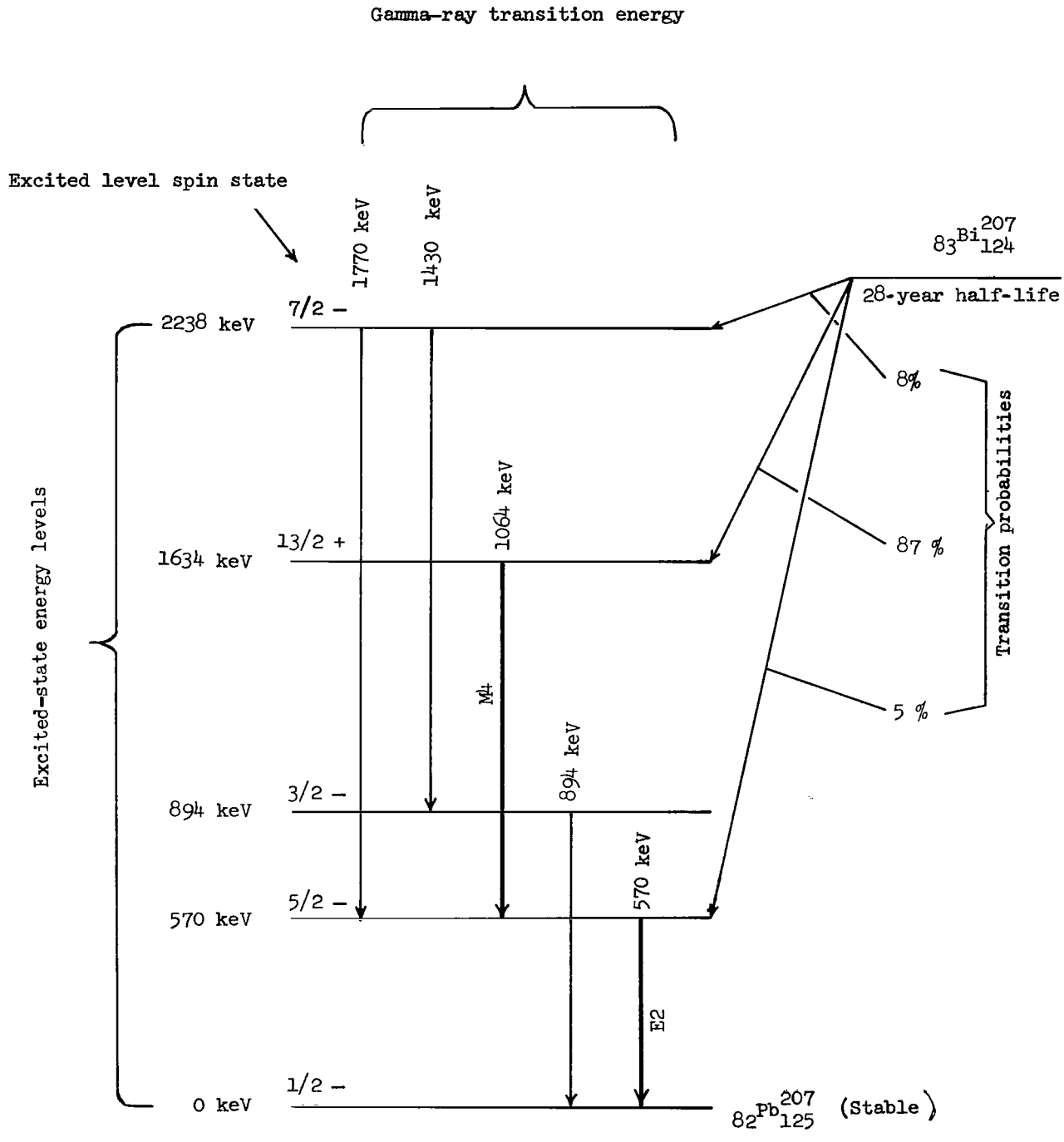

Figure 3.- Decay scheme of bismuth-207. (M4 is a transition for which the selection rule is $\Delta I = 4$, yes; E2 is a transition for which the selection rule is $\Delta I = 2$, no.)

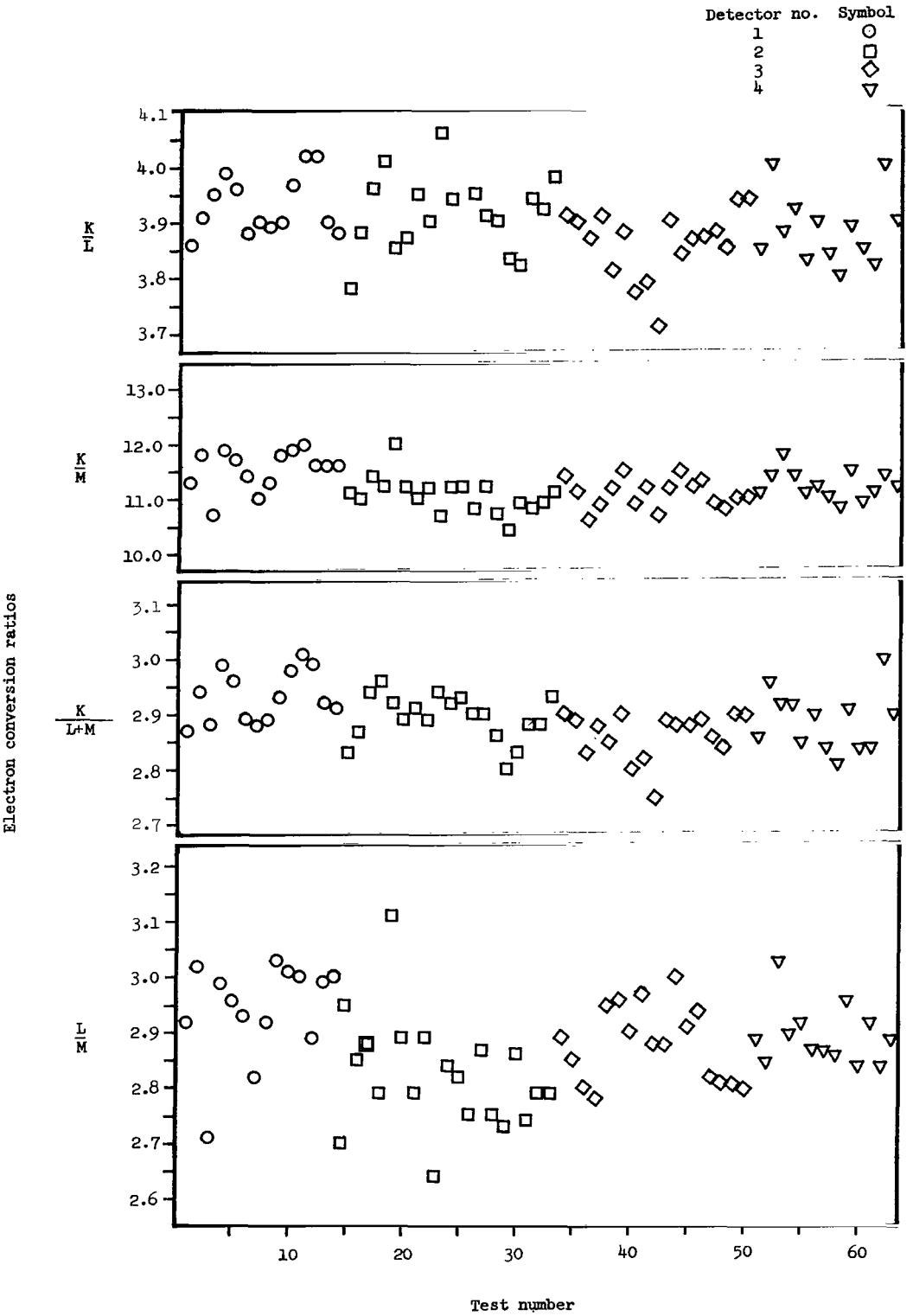

Figure 4.- Measured conversion ratios. (All data from the four detectors are shown.)

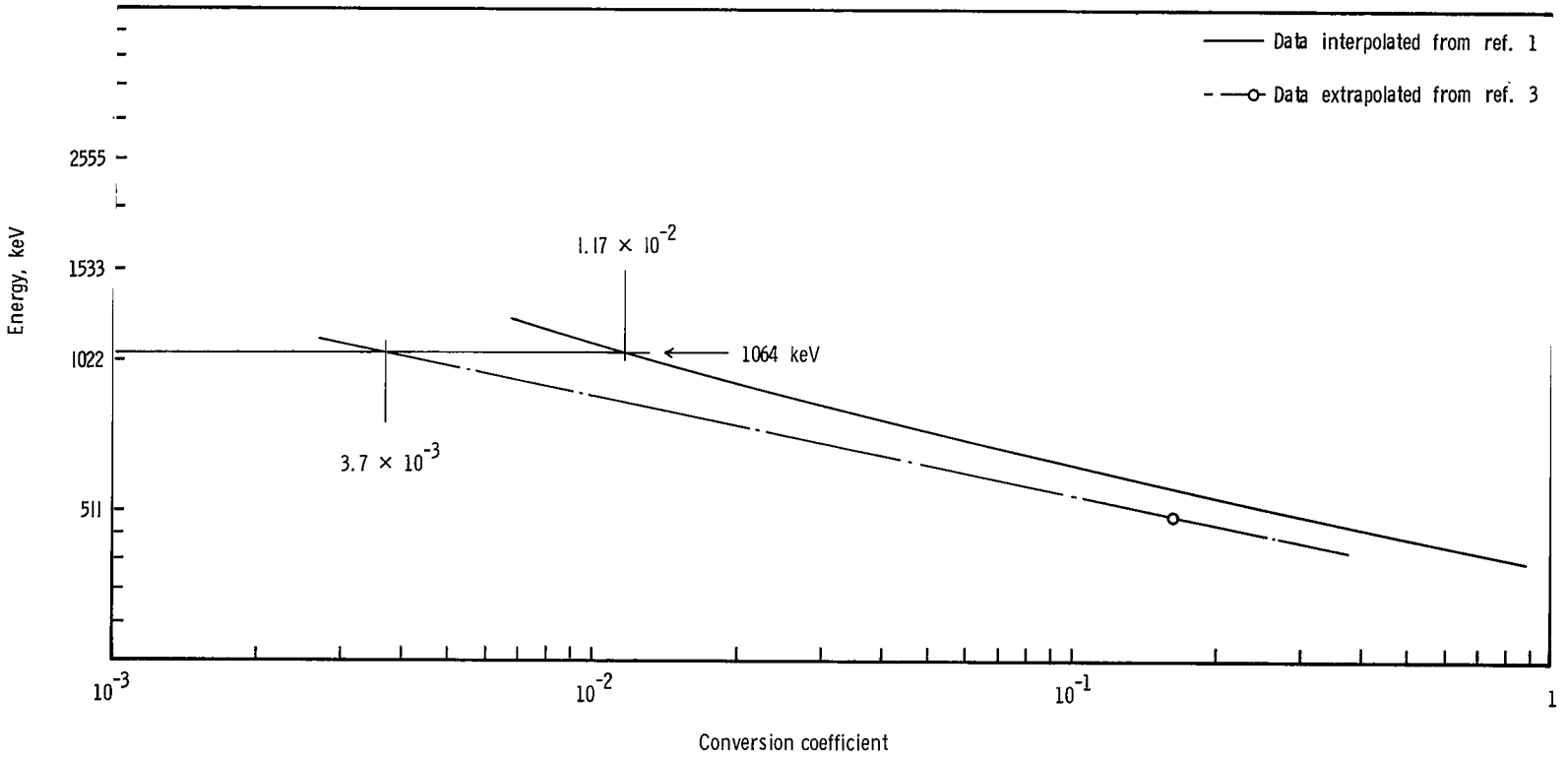

Figure 5.- Total M-shell internal conversion coefficient.

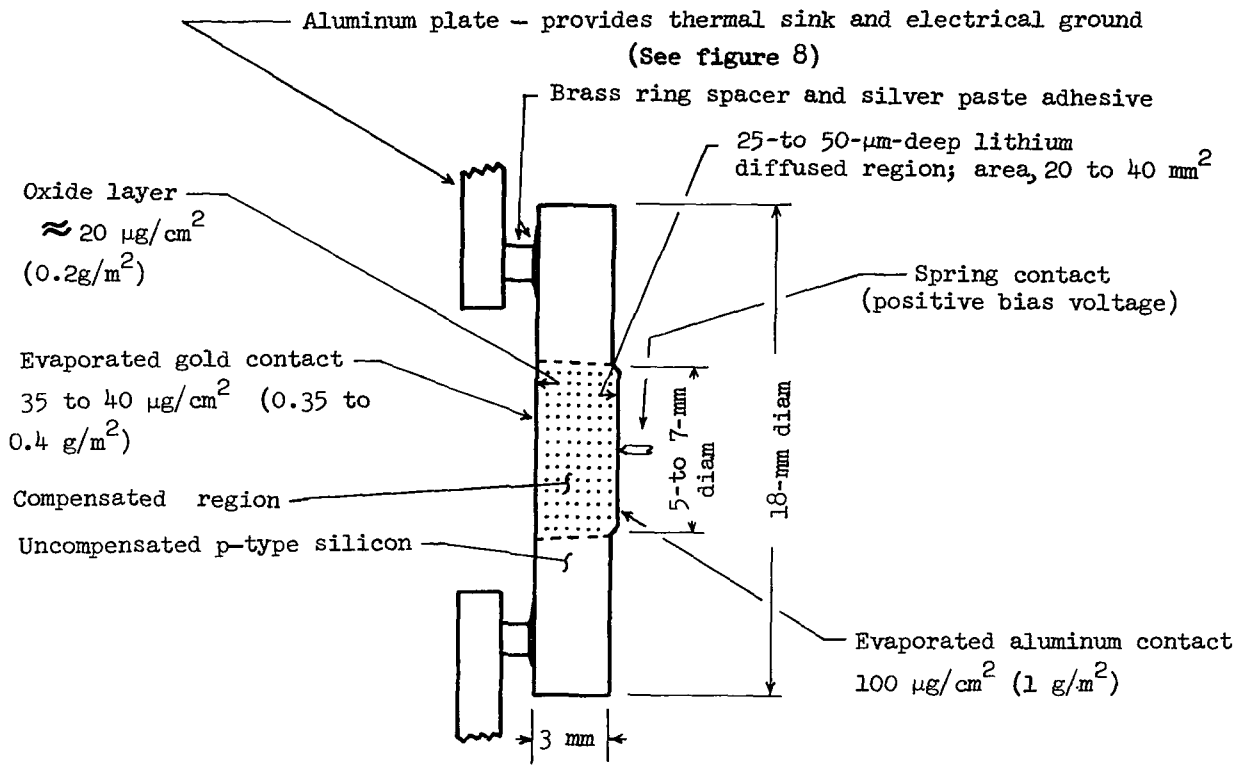

Detector characteristics:

Silicon: p-type, boron doped, float zoned, (1,1,1) orientation

Resistivity: 10 000 Ω - cm (10 kΩ-cm)

Minority carrier lifetime: ≥ 1 ms

Dislocation density: < 30 000 etch pits/cm²

Leakage current at 77 K ≈ 10^{-11} ampere at 500 volts

Capacitance ≈ 10 pF

Active area: 20 to 40 mm²

Figure 6.- Detector characteristics.

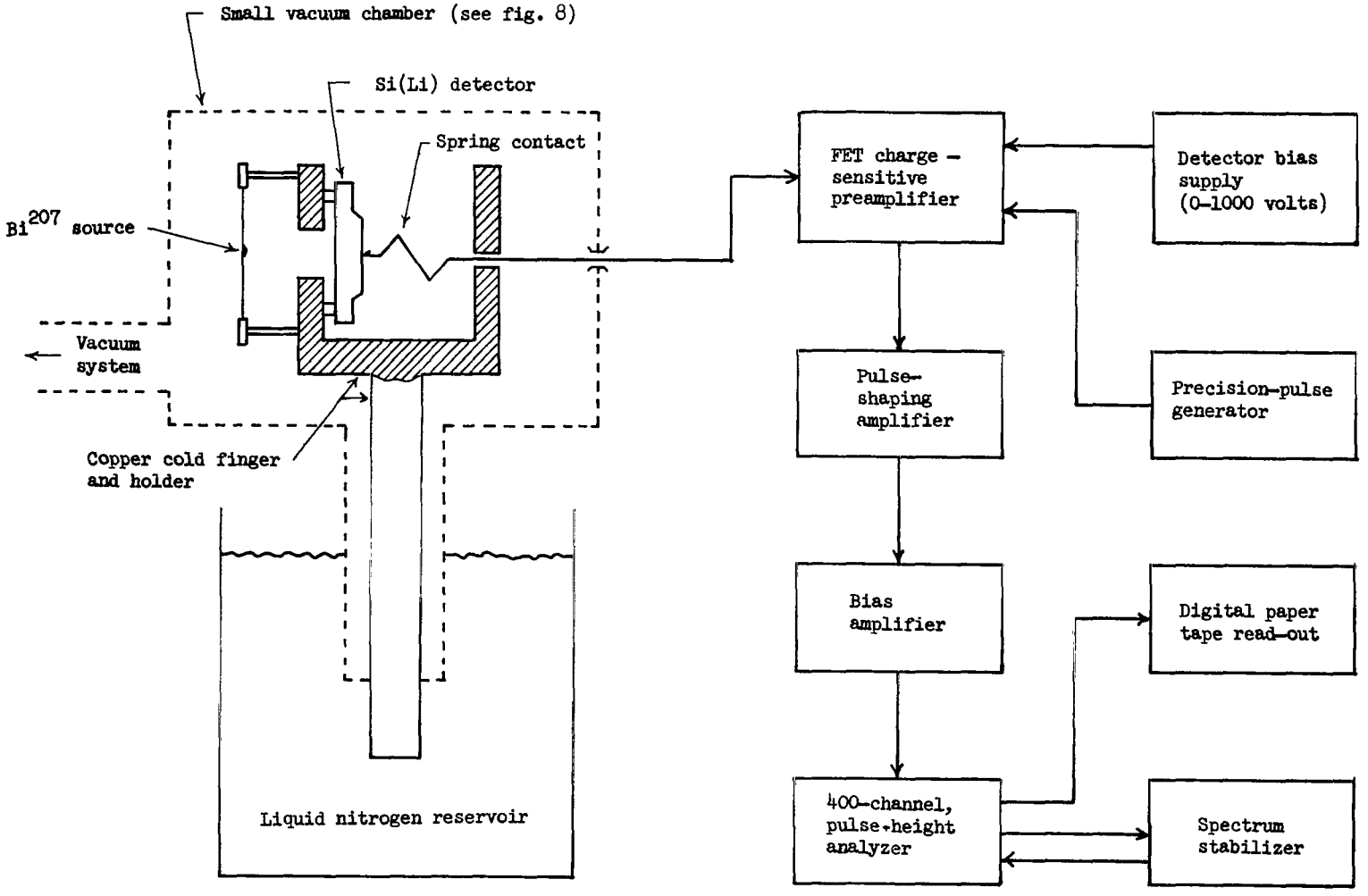

Figure 7.- Apparatus for determining detector energy resolution.

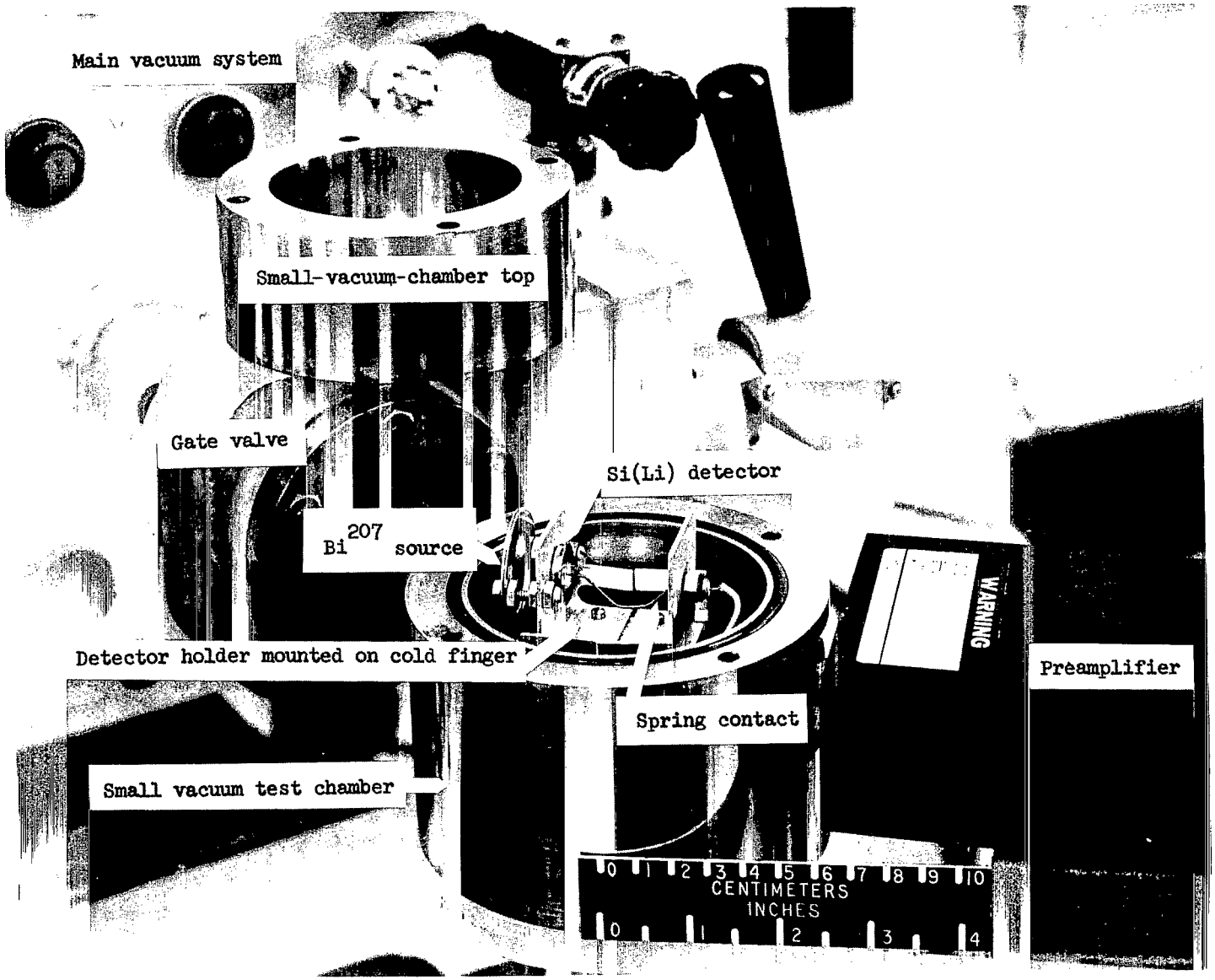

Figure 8.- Details of detector and source holder.

L-68-9168.1

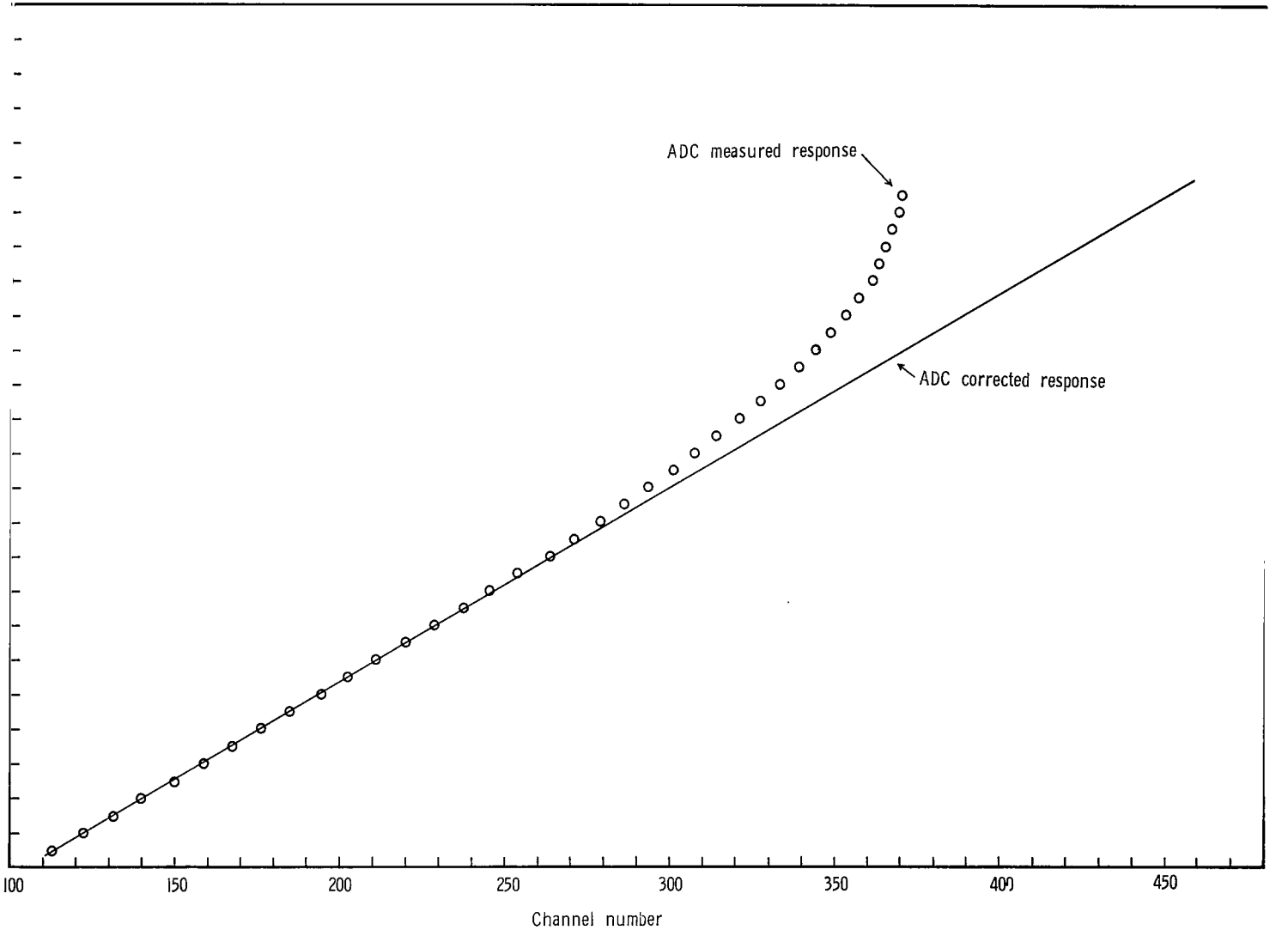

Figure 9.- Dependence of channel location on input-pulse amplitude.

"The aeronautical and space activities of the United States shall be conducted so as to contribute . . . to the expansion of human knowledge of phenomena in the atmosphere and space. The Administration shall provide for the widest practicable and appropriate dissemination of information concerning its activities and the results thereof."

—NATIONAL AERONAUTICS AND SPACE ACT OF 1958

NASA SCIENTIFIC AND TECHNICAL PUBLICATIONS

TECHNICAL REPORTS: Scientific and technical information considered important, complete, and a lasting contribution to existing knowledge.

TECHNICAL NOTES: Information less broad in scope but nevertheless of importance as a contribution to existing knowledge.

TECHNICAL MEMORANDUMS: Information receiving limited distribution because of preliminary data, security classification, or other reasons.

CONTRACTOR REPORTS: Scientific and technical information generated under a NASA contract or grant and considered an important contribution to existing knowledge.

TECHNICAL TRANSLATIONS: Information published in a foreign language considered to merit NASA distribution in English.

SPECIAL PUBLICATIONS: Information derived from or of value to NASA activities. Publications include conference proceedings, monographs, data compilations, handbooks, sourcebooks, and special bibliographies.

TECHNOLOGY UTILIZATION PUBLICATIONS: Information on technology used by NASA that may be of particular interest in commercial and other non-aerospace applications. Publications include Tech Briefs, Technology Utilization Reports and Notes, and Technology Surveys.

Details on the availability of these publications may be obtained from:

SCIENTIFIC AND TECHNICAL INFORMATION DIVISION

NATIONAL AERONAUTICS AND SPACE ADMINISTRATION

Washington, D.C. 20546